Published in final edited form as:
Pediatr Blood Cancer. 2010 October ; 55(4): 668–677. doi:10.1002/pbc.22576.

Initial Testing (Stage 1) of AZD6244 (ARRY-142886) by the Pediatric Preclinical Testing Program

E. Anders Kolb, MD[1], **Richard Gorlick, MD**[2], **Peter J. Houghton, PhD**[3], **Christopher L. Morton, BS**[3], **Geoffrey Neale, PhD**[3], **Stephen T. Keir, PhD**[4], **Hernan Carol, PhD**[5], **Richard Lock, PhD**[5], **Doris Phelps, BS**[3], **Min H. Kang, PharmD**[6], **C. Patrick Reynolds, MD, PhD**[6], **John M. Maris, MD**[7], **Catherine Billups, MS**[3], and **Malcolm A. Smith, MD, PhD**[8]

[1] A.I. duPont Hospital for Children, Wilmington, DE.

[2] The Children's Hospital at Montefiore, Bronx, NY.

[3] St. Jude Children's Research Hospital, Memphis, TN.

[4] Duke University Medical Center, Durham, NC.

[5] Children's Cancer Institute Australia for Medical Research, Randwick, NSW, Australia.

[6] Children's Hospital of Los Angeles, Los Angeles, CA.

[7] Children's Hospital of Philadelphia, University of Pennsylvania School of Medicine and Abramson Family Cancer Research Institute, Philadelphia, PA.

[8] Cancer Therapy Evaluation Program, NCI, Bethesda, MD.

Abstract

Background—AZD6244 (ARRY-142886) is a potent small molecule inhibitor of MEK1/2 that is in phase 2 clinical development.

Procedures—AZD6244 was tested against the PPTP *in vitro* panel (1 nM-10μM). *In vivo* AZD6244 was tested at a dose of 100 mg/kg administered orally twice daily five days per week for 6 weeks. Subsequently, AZD6244 was evaluated against two juvenile pilocytic astrocytoma (JPA) xenografts using once and twice daily dosing schedules. Phosphorylation of ERK1/2 was used as a surrogate for *in vivo* inhibition of MEK1/2 was determined by immunoblotting.

Results—At the highest concentration used *in vitro* (10 μM) AZD6244 only inhibited growth by 50% in 5 of the 23 cell lines. Against the *in vivo* tumor panels, AZD6244 induced significant differences in EFS distribution in 10 of 37 (27%) solid tumor models and 0 of 6 acute lymphoblastic leukemia (ALL) models. There were no objective responses. Pharmacodynamic studies indicated at this dose and schedule AZD6244 completely inhibited ERK1/2 phosphorylation. AZD6244 was evaluated against two JPA xenografts, BT-35 (wild type BRAF) and BT-40 (mutant [V600E] BRAF). BT-40 xenografts were highly sensitive to AZD6244, whereas BT-35 xenografts progressed on AZD6244 treatment.

Conclusions—At the dose and schedule of administration used, AZD6244 as a single agent had limited *in vitro and in vivo* activity against the PPTP tumor panels despite inhibition of MEK1/2 activity. However, AZD6244 was highly active against BT-40 JPA xenografts that harbor constitutively activated BRAF, causing complete regressions.

Corresponding Author: E. Anders Kolb, M.D. A.I. duPont Hospital for Children 1600 Rockland Road Wilmington, DE 19803 Voice: 302-651-5567 eakolb@nemours.org.

Conflict of interest statement: The authors consider that there are no actual or perceived conflicts of interest.

Keywords

Preclinical Testing; Developmental Therapeutics; AZD6244

INTRODUCTION

MEK1 and MEK2 (mitogen-activated protein kinase kinase) are dual-specificity protein kinases that function in a mitogen activated protein kinase (MAPK) cascade controlling cell proliferation and differentiation. MEK1/2 activate the extracellular signal-regulated kinases 1 and 2 (ERK 1/2), which have wide substrate specificity, resulting in activation of a multitude of cellular responses involved in control of growth, differentiation and apoptosis.

Constitutive activation of the MAPK pathway in human tumors is a common event. Activation may occur through multiple mechanisms, including gain-of-function mutations in RAS family members and BRAF [1] and through activation of growth factor signaling. Over 40 missense mutations have been identified in the BRAF gene, among which the 1799A point mutation in exon 15 accounts for up to 90% [2]. This mutation causes a V600E amino-acid substitution in codon 600 and converts BRAF into a constitutively activated dominant transforming protein kinase, BRAFV600E, which causes cancer through aberrant activation of the Ras/Raf/MEK/MAP kinase/ERK signaling pathway (MAP kinase pathway). However mutations of BRAF as a mechanism of tumorigenesis in childhood solid cancers appears to be rare [3] as no mutations were found in 181 childhood tumors including neuroblastoma, Wilms tumor, hepatoblastoma, teratoma, rhabdomyosarcoma and ganglioneuroma. Similarly, no evidence for oncogenic mutations affecting NRAS, KRAS, HRAS, BRAF were identified in medulloblastoma [4]. In contrast mutations of BRAF and NRAS appear more frequently in childhood acute lymphoblastic leukemia (ALL) [5,6]. More recently, tandem duplication producing a novel fusion gene (KIAA1549-BRAF) that lacks the BRAF regulatory domain has been described in juvenile pilocytic astrocytomas (JPA) [7-10], whereas activating mutations in JPA are less frequent, being identified in approximately 5 percent of cases.

As the primary activator of ERK 1/2, MEK1/2 is a compelling target for anti-neoplastic therapy [2,11]. AZD6244 (ARRY-142886) is a potent and selective inhibitor of MEK 1/2 kinases [12-14] that is currently in phase II clinical development [15,16]. Given the selectivity of AZD6244 for MEK 1/2 [13,14], the Pediatric Preclinical Testing Program (PPTP) evaluated this agent to gain insight into the utility of specifically targeting the MAPK pathway in pediatric tumors.

MATERIALS AND METHODS

In vitro testing

In vitro testing was performed using DIMSCAN, a semiautomatic fluorescence-based digital image microscopy system that quantifies viable (using fluorescein diacetate [FDA]) cell numbers in tissue culture multiwell plates [17]. Cells were incubated in the presence of AZD6244 for 96 hours at concentrations from 1 nM to 10 μM and analyzed as previously described [18].

In vivo tumor growth inhibition studies

CB17SC-M *scid*$^{-/-}$ female mice (Taconic Farms, Germantown NY), were used to propagate subcutaneously implanted kidney/rhabdoid tumors, sarcomas (Ewing, osteosarcoma, rhabdomyosarcoma), neuroblastoma, and non-glioblastoma brain tumors, while BALB/c nu/

nu mice were used for glioma models, as previously described [19-21]. Human leukemia cells were propagated by intravenous inoculation in female non-obese diabetic (NOD)/*scid*$^{-/-}$ mice as described previously [22]. Female mice were used irrespective of the gender of the patient from which the tumor was derived. All mice were maintained under barrier conditions and experiments were conducted using protocols and conditions approved by the institutional animal care and use committee of the appropriate consortium member. Ten mice were used per group for solid tumors and 8 mice per group were used for ALL models. Tumor volumes (cm^3) [solid tumor xenografts] or percentages of human CD45-positive [hCD45] cells [ALL xenografts] were determined as previously described [23]. Responses were determined using three activity measures as previously described [23]. An in-depth description of the analysis methods is included in the Supplemental Response Definitions section.

Statistical Methods

The exact log-rank test, as implemented using Proc StatXact for SAS®, was used to compare event-free survival distributions between treatment and control groups. P-values were two-sided and were not adjusted for multiple comparisons given the exploratory nature of the studies.

Drugs and Formulation

AZD6244 was provided to the Pediatric Preclinical Testing Program by AstraZeneca through the Cancer Therapy Evaluation Program (NCI). AZD6244 was dissolved in 0.5% hydroxypropyl methyl cellulose, 0.1% Polysorbate 80 and administered p.o., using a twice daily schedule (excepting weekends, for which a once daily (SID) schedule was used) for 6 weeks at a dose of 100 mg/kg. AZD6244 was provided to each consortium investigator in coded vials for blinded testing.

Pharmacodynamic studies

MEK1/2 inhibition was determined by assaying phosphorylation of ERK1/2 by immunoblotting. Mice bearing OS-33 xenografts were treated with either vehicle or AZD6244 at 100mg/kg BID for 5 days. Tumors were harvested 1 hour after the first dose on day 5 [24]. Tumors were excised, snap frozen and analyzed for phospho-ERK1/2 using anti-phospho ERK1/2(Thr202/Tyr204) antibody (Cell Signaling, Beverly, MA) by Western blot analysis as described previously [24].

BRAF sequencing

The genomic DNA from BT-35 and BT-40 was screened for BRAF mutations with primers designed to amplify the exons 1-18 using primers described previously [1]. Big Dye Terminator Chemistry was used for sequencing.

FISH analysis

Purified BRAF BAC DNA was labeled with digoxigenin-11-dUTP (Roche Molecular Biochemicals, Indianapolis, IN) by nick translation. The labeled probe was combined with sheared mouse DNA and independently hybridized to interphase nuclei derived from the 3 samples in a solution containing 50% formamide, 10% dextran sulfate, and 2X SSC. Probe-detection was performed by incubating the hybridized slides in fluorescein-labeled anti-digoxigenin (Roche Molecular Biochemicals).

Affymetrix SNP6.0 array analysis

DNA was extracted from xenograft samples using DNeasy Tissue kit (Qiagen). Microarray analysis of genomic DNA was done in the Hartwell Center Core Laboratory using the

Affymetrix Genome-Wide Human 6.0 SNP array, containing ~1.8 million markers throughout the genome, according to the standard Affymetrix protocol. Copy number analysis and segmentation were performed using the CNATv5 algorithm as implemented in the Affymetrix Genotyping Console v 3.01. Tumor DNA was compared to a diploid reference set comprising 129 St. Jude Children's Research Hospital acute lymphoblastic leukemia remission samples. The Hidden Markov model in the CNATv5 algorithm was used to infer copy number and to identify genomic gains and losses. Segments with aberrant copy number were identified only if they consisted of at least 10 consecutive markers and comprised a minimum size of 100kb.

RESULTS

In vitro testing

AZD6244 inhibited growth in a minority of the cell lines from the PPTP *in vitro* panel. Kasumi-1, a cell line with an activating mutation in KIT, was the most responsive cell line and the only cell line with a clear cytotoxic response to AZD6244. Four of the remaining 22 cell lines achieved at least 50% growth inhibition, including two rhabdomyosarcoma cell lines (RD and Rh18), a neuroblastoma cell line (NB-EBc1), and a T-cell ALL cell line (MOLT-4) (Table 1). The distribution of IC_{50} values and examples of responses for Kasumi-1 and NB-EBc1 are shown in Figure 1.

In vivo testing

AZD6244 was evaluated in 44 xenograft models and was well tolerated at the dose and schedule used for *in vivo* testing. Eleven of 842 mice died during the study (1.3%), with 0 of 420 in the control arms (0%) and 11 of 428 in the AZD6244 treatment arms (2.6%). One line (ALL-17) was excluded from analysis due to toxicity greater than 25 percent. A complete summary of results is provided in Supplemental Table I, including total numbers of mice, number of mice that died (or were otherwise excluded), numbers of mice with events and average times to event, tumor growth delay, as well as numbers of responses and T/C values.

AZD6244 induced significant differences in EFS distribution compared to controls in 10 of 43 evaluable xenografts (Table II). Significant differences in EFS distribution occurred in the majority of xenografts in the glioblastoma panel (3 of 4) and in one-half of the xenografts from the osteosarcoma panel (3 of 6), but in none of the evaluable xenografts in the Ewing, Wilms, medulloblastoma, and ALL panels. The *in vivo* testing results for the objective response measure of activity are presented in Figure 2 in a 'heat-map' format as well as a 'COMPARE'-like format, based on the scoring criteria described in the Material and Methods and the Supplemental Response Definitions section. The latter analysis demonstrates relative tumor sensitivities around the midpoint score of 5 (stable disease). No objective responses (defined as ≥ 50% tumor volume regression) were observed in any of the models. The best responses observed were nine examples of PD2 (progressive disease with growth delay). These included 2 of 4 glioblastoma xenografts (BT-39 and D645) and 3 or 6 osteosarcoma xenografts (OS-1, OS-17, and OS-33). Examples of typical solid tumor response shown in Figure 3 for two osteosarcoma xenografts (OS-1 and OS-33) and one glioblastoma xenograft (BT-39) that met the criteria for intermediate activity (EFS T/C value > 2.0 and a significant difference in EFS distribution) for the time to event (EFS T/C) activity measure used by the PPTP. AZD6244 markedly reduced ERK phosphorylation in the responsive osteosarcoma xenograft OS-33, confirming the expected pharmacodynamic effect for AZD6244 at the dose employed for testing (Figure 4).

The PPTP has established two models of JPA (BT-35 and BT-40) for use in secondary tumor panels. Both xenografts were evaluated for copy number alterations using Affymetrix SNP6.0 arrays. BT-35 and BT-40 showed no evidence for focal gain in the region of the BRAF gene, while BT-40 demonstrated gain of the entire long arm of chromosome 7 (Figure 5). These observations support absence of the KIAA1549/BRAF fusion in these xenografts. Fluorescence in situ hybridization (FISH) using probes for BRAF and for the chromosome 7 centromere showed equal numbers of these probes (Figure 6A), supporting the absence of focal BRAF duplication in the xenografts. By FISH analysis there were 5-8 copies of chromosome 7 in cells derived from BT-35 and 4-5 copies in cells derived from BT-40 tumors (Figure 6A). Sequencing showed that BRAF is wild type in BT-35, whereas BT-40 has a mutant (V600E) activating mutation (Figure 6B). AZD6244 was evaluated against these two models at 100 or 75 mg/kg (BID × 5 and once daily (SID) × 2) per week, or 100 mg/kg daily × 7 for 6 consecutive weeks (Supplemental Table 2). BT-35 xenografts were intrinsically resistant to AZD6244 (Figure 7A) whereas BT-40 xenografts were highly sensitive to each treatment schedule demonstrating CR at the end of treatment (6 weeks) Figure 7B. The delay in tumor re-growth, after stopping therapy, was related to the cumulative dose of AZD6244 received.

DISCUSSION

For the PPTP *in vitro* panel, 50% growth inhibition by AZD6244 was achieved in only 5 of 23 tumor lines. The most responsive cell line, Kasumi-1, has an activating KIT mutation [25], and its response to AZD6244 is similar to that previously described for selected BRAF and RAS mutant adult cancer cell lines [13,14]. Among the remaining PPTP cell lines, BRAF and RAS mutational status is known for 10 and 8 cell lines, respectively (Table 1). Mutations in BRAF were not observed. Two of 3 cell lines with activating RAS mutations achieved 50% growth inhibition, while only Kasumi-1 among the cell lines with known wild type RAS status achieved 50% growth inhibition.

AZD6244 demonstrated limited single agent *in vivo* activity against the PPTP's childhood cancer models. The best response was progressive disease with significant tumor growth inhibition. Significant tumor growth inhibition was most consistently observed for the osteosarcoma (3 of 6) and glioblastoma (3 of 4) tumor panels.

Mutations in BRAF are associated with an increased sensitivity to MEK inhibition, while the response of cell lines with RAS gene mutations is more variable with both sensitivity and resistance observed [11,13,14]. BRAF mutations are uncommon in pediatric sarcomas [3], renal tumors [3], neuroblastoma [3,26], glioblastoma [27], and medulloblastoma [4], and are found in only 10% of childhood ALL [5]. This infrequency of BRAF mutation likely contributes to the relative insensitivity of most of the PPTP tumor lines to MEK1/2 inhibition. Pilocytic astrocytomas are reported to have MAPK pathway activation through BRAF activating mutations and through a tandem duplication that results in an in-frame fusion between the 5′ end of the KIAA1549 gene and the 3′ end of the BRAF gene producing an oncogenic fusion protein [9,28]. Two juvenile pilocytic astrocytoma xenografts have been established as secondary models within the PPTP. Neither line showed evidence for BRAF duplication, but direct sequencing of BRAF identified a well-characterized activating mutation (V600E) in BT-40 tumor tissue. The sensitivity of these tumors to treatment with AZD6244 was examined using two dose levels and schedules. BT-40 xenografts were sensitive to all treatments demonstrating a complete response at both dose levels on the BID schedule, but less sensitivity on the SID schedule. This result is consistent with a complete maintained response reported in a patient with this activating mutation in a melanoma [16]. In contrast, BT-35 xenografts were not sensitive to either dose/schedule of AZD6244 administration. Further dose-response testing (50 and 25 mg/kd

BID) that may more readily simulate drug exposures achieved in the clinic using the hydrogen sulfate capsules [16] will be needed to determine whether tumor regressions for BT-40 occur at doses that produce drug exposures closer to those in the clinical setting.

The MEK1/2 inhibitor AZD6244, was not effective in inducing regressions as a single agent against most of the pediatric preclinical models evaluated. Both MEK1 mutations [29] or Ras effector signaling through PI3 kinase have been implicated in resistance to AZD6244 [29,30]. However, more recent data suggest a more complex mechanism by which cells are intrinsically resistant or sensitive to this agent, where expression of the compensatory-resistance expression signature appeared independent of PI3 kinase pathway activation [16]. AZD6244 may show greater benefit in combination with inhibitors of other signaling pathways (e.g., mTOR inhibitors) [31], where combined inhibition of mTOR and the Ras/MAPK pathways inhibited ribosome biogenesis and protein translation more effectively than either agent alone. Further, inhibition of MEK1 signaling appears to be the mechanism accounting for synergy between lapatinib and radiation [32] and AZD6244 was synergistic when combined with chemotherapeutic agents such as docetaxel [33]

The relative sensitivity of osteosarcoma and glioblastoma xenografts to AZD6244 suggests that preclinical combination testing in these histologic subsets may be worthwhile. The complete regressions induced by AZD6244 against a BRAF-mutant pilocytic astrocytoma xenograft are a strong activity signal that points to the potential utility of MEK inhibition for this tumor type.

Supplementary Material

Refer to Web version on PubMed Central for supplementary material.

Acknowledgments

This work was supported by NO1-CM-42216, CA21765, and CA108786 from the National Cancer Institute, and AZD6244 was provided by AstraZeneca. In addition to the authors, the manuscript represents work contributed by the following: Sherry Ansher, Joshua Courtright, Edward Favours, Henry S. Friedman, Debbie Payne-Turner, Charles Stopford, Mayamin Tajbakhsh, Chandra Tucker, Jianrong Wu, Joe Zeidner, Ellen Zhang, and Jian Zhang. Children's Cancer Institute Australia for Medical Research is affiliated with the University of New South Wales and Sydney Children's Hospital. We gratefully acknowledge the assistance of Marc Valentine, Cancer Center Core Cytogenetic Laboratory at St. Jude Children's Research Hospital for FISH analysis.

Reference List

1. Davies H, Bignell GR, Cox C, et al. Mutations of the BRAF gene in human cancer. Nature. 2002; 417(6892):949–954. [PubMed: 12068308]
2. Garnett MJ, Marais R. Guilty as charged: B-RAF is a human oncogene. Cancer Cell. 2004; 6(4): 313–319. [PubMed: 15488754]
3. Miao J, Kusafuka T, Fukuzawa M. Hotspot mutations of BRAF gene are not associated with pediatric solid neoplasms. Oncol Rep. 2004; 12(6):1269–1272. [PubMed: 15547749]
4. Gilbertson RJ, Langdon JA, Hollander A, et al. Mutational analysis of PDGFR-RAS/MAPK pathway activation in childhood medulloblastoma. Eur J Cancer. 2006; 42(5):646–649. [PubMed: 16434186]
5. Gustafsson B, Angelini S, Sander B, et al. Mutations in the BRAF and N-ras genes in childhood acute lymphoblastic leukaemia. Leukemia. 2005; 19(2):310–312. [PubMed: 15538400]
6. Case M, Matheson E, Minto L, et al. Mutation of genes affecting the RAS pathway is common in childhood acute lymphoblastic leukemia. Cancer Res. 2008; 68(16):6803–6809. [PubMed: 18701506]

7. Jones DT, Kocialkowski S, Liu L, et al. Tandem duplication producing a novel oncogenic BRAF fusion gene defines the majority of pilocytic astrocytomas. Cancer Res. 2008; 68(21):8673–8677. [PubMed: 18974108]
8. Jones DT, Kocialkowski S, Liu L, et al. Oncogenic RAF1 rearrangement and a novel BRAF mutation as alternatives to KIAA1549:BRAF fusion in activating the MAPK pathway in pilocytic astrocytoma. Oncogene. 2009
9. Pfister S, Janzarik WG, Remke M, et al. BRAF gene duplication constitutes a mechanism of MAPK pathway activation in low-grade astrocytomas. The Journal of clinical investigation. 2008; 118(5): 1739–1749. [PubMed: 18398503]
10. Forshew T, Tatevossian RG, Lawson AR, et al. Activation of the ERK/MAPK pathway: a signature genetic defect in posterior fossa pilocytic astrocytomas. J Pathol. 2009; 218(2):172–181. [PubMed: 19373855]
11. Solit DB, Garraway LA, Pratilas CA, et al. BRAF mutation predicts sensitivity to MEK inhibition. Nature. 2006; 439(7074):358–362. [PubMed: 16273091]
12. Wan PT, Garnett MJ, Roe SM, et al. Mechanism of activation of the RAF-ERK signaling pathway by oncogenic mutations of B-RAF. Cell. 2004; 116(6):855–867. [PubMed: 15035987]
13. Davies BR, Logie A, McKay JS, et al. AZD6244 (ARRY-142886), a potent inhibitor of mitogen-activated protein kinase/extracellular signal-regulated kinase kinase 1/2 kinases: mechanism of action in vivo, pharmacokinetic/pharmacodynamic relationship, and potential for combination in preclinical models. Molecular cancer therapeutics. 2007; 6(8):2209–2219. [PubMed: 17699718]
14. Yeh TC, Marsh V, Bernat BA, et al. Biological characterization of ARRY-142886 (AZD6244), a potent, highly selective mitogen-activated protein kinase kinase 1/2 inhibitor. Clin Cancer Res. 2007; 13(5):1576–1583. [PubMed: 17332304]
15. Adjei AA, Cohen RB, Franklin W, et al. Phase I pharmacokinetic and pharmacodynamic study of the oral, small-molecule mitogen-activated protein kinase kinase 1/2 inhibitor AZD6244 (ARRY-142886) in patients with advanced cancers. J Clin Oncol. 2008; 26(13):2139–2146. [PubMed: 18390968]
16. Banerji U, Camidge DR, Verheul HM, et al. The first-in-human study of the hydrogen sulfate (Hyd-sulfate) capsule of the MEK1/2 inhibitor AZD6244 (ARRY-142886): a phase I open-label multicenter trial in patients with advanced cancer. Clin Cancer Res. 16(5):1613–1623. [PubMed: 20179232]
17. Frgala T, Kalous O, Proffitt RT, et al. A fluorescence microplate cytotoxicity assay with a 4-log dynamic range that identifies synergistic drug combinations. Molecular cancer therapeutics. 2007; 6(3):886–897. [PubMed: 17363483]
18. Houghton PJ, Morton CL, Kolb EA, et al. Initial testing (stage 1) of the proteasome inhibitor bortezomib by the pediatric preclinical testing program. Pediatr Blood Cancer. 2007
19. Friedman HS, Colvin OM, Skapek SX, et al. Experimental chemotherapy of human medulloblastoma cell lines and transplantable xenografts with bifunctional alkylating agents. Cancer research. 1988; 48(15):4189–4195. [PubMed: 3390813]
20. Graham C, Tucker C, Creech J, et al. Evaluation of the antitumor efficacy, pharmacokinetics, and pharmacodynamics of the histone deacetylase inhibitor depsipeptide in childhood cancer models in vivo. Clin Cancer Res. 2006; 12(1):223–234. [PubMed: 16397046]
21. Peterson JK, Tucker C, Favours E, et al. In vivo evaluation of ixabepilone (BMS247550), a novel epothilone B derivative, against pediatric cancer models. Clin Cancer Res. 2005; 11(19 Pt 1): 6950–6958. [PubMed: 16203787]
22. Liem NL, Papa RA, Milross CG, et al. Characterization of childhood acute lymphoblastic leukemia xenograft models for the preclinical evaluation of new therapies. Blood. 2004; 103(10):3905–3914. [PubMed: 14764536]
23. Houghton PJ, Morton CL, Tucker C, et al. The pediatric preclinical testing program: Description of models and early testing results. Pediatr Blood Cancer. 2006
24. Kurmasheva RT, Harwood FC, Houghton PJ. Differential regulation of vascular endothelial growth factor by Akt and mammalian target of rapamycin inhibitors in cell lines derived from childhood solid tumors. Mol Cancer Ther. 2007; 6(5):1620–1628. [PubMed: 17483438]

25. Beghini A, Magnani I, Ripamonti CB, et al. Amplification of a novel c-Kit activating mutation Asn(822)-Lys in the Kasumi-1 cell line: a t(8;21)-Kit mutant model for acute myeloid leukemia. Hematol J. 2002; 3(3):157–163. [PubMed: 12111653]

26. Dam V, Morgan BT, Mazanek P, et al. Mutations in PIK3CA are infrequent in neuroblastoma. BMC cancer. 2006; 6:177. [PubMed: 16822308]

27. Knobbe CB, Reifenberger J, Reifenberger G. Mutation analysis of the Ras pathway genes NRAS, HRAS, KRAS and BRAF in glioblastomas. Acta Neuropathol. 2004; 108(6):467–470. [PubMed: 15517309]

28. Jones, DT.; Kocialkowski, S.; Liu, L., et al. A novel oncogenic fusion gene is found in the majority of pilocytic astrocytomas. Proceedings of the 99th Annual Meeting of the American Association for Cancer Research; 2008.

29. Emery CM, Vijayendran KG, Zipser MC, et al. MEK1 mutations confer resistance to MEK and B-RAF inhibition. Proc Natl Acad Sci U S A. 2009; 106(48):20411–20416. [PubMed: 19915144]

30. Wee S, Jagani Z, Xiang KX, et al. PI3K pathway activation mediates resistance to MEK inhibitors in KRAS mutant cancers. Cancer Res. 2009; 69(10):4286–4293. [PubMed: 19401449]

31. Legrier ME, Yang CP, Yan HG, et al. Targeting protein translation in human non small cell lung cancer via combined MEK and mammalian target of rapamycin suppression. Cancer research. 2007; 67(23):11300–11308. [PubMed: 18056456]

32. Sambade MJ, Camp JT, Kimple RJ, et al. Mechanism of lapatinib-mediated radiosensitization of breast cancer cells is primarily by inhibition of the Raf>MEK>ERK mitogen-activated protein kinase cascade and radiosensitization of lapatinib-resistant cells restored by direct inhibition of MEK. Radiother Oncol. 2009; 93(3):639–644. [PubMed: 19853943]

33. Haass NK, Sproesser K, Nguyen TK, et al. The mitogen-activated protein/extracellular signal-regulated kinase kinase inhibitor AZD6244 (ARRY-142886) induces growth arrest in melanoma cells and tumor regression when combined with docetaxel. Clin Cancer Res. 2008; 14(1):230–239. [PubMed: 18172275]

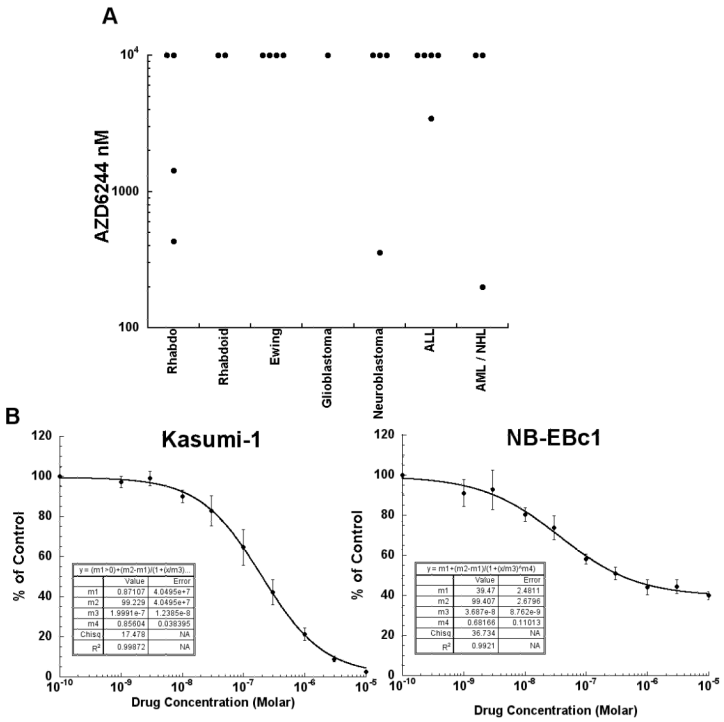

Figure 1.

AZD6244 *in vitro* activity. Panel A is a dot plot chart that illustrates the relative sensitivity of the cell lines using the IC_{50} values displayed by histology. Panel B illustrates typical growth inhibition curves for Kasumi-1 and NB-EBc1. Error bars represent standard deviations for each concentration tested.

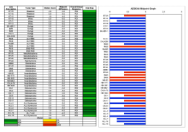

Figure 2.

AZD6244 *in vivo* objective response activity. Left: The colored ‘heat map’ depicts group response scores. A high level of activity is indicated by a score of 6 or more, intermediate activity by a score of ≥ 2 but < 6, and low activity by a score of < 2. Right: representation of tumor sensitivity based on the difference of individual tumor lines from the midpoint response (stable disease). Bars to the right of the median represent lines that are more sensitive, and to the left are tumor models that are less sensitive. Red bars indicate lines with a significant difference in EFS distribution between treatment and control groups, while blue bars indicate lines for which the EFS distributions were not significantly different.

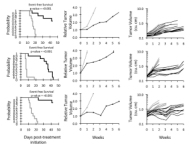

Figure 3.

AZD6244 activity against individual solid tumor xenografts, Kaplan-Meier curves for EFS, median relative tumor volume graphs, and individual tumor volume graphs are shown for selected lines: (A) OS-1 (B) OS-33, and (C) BT-39. Mice received AZD6244 (100 mg/kg BID x 5 (Monday-Friday) and once daily (SID) (Saturday-Sunday) [abbreviated BID × 5/ SID × 2] for six consecutive weeks

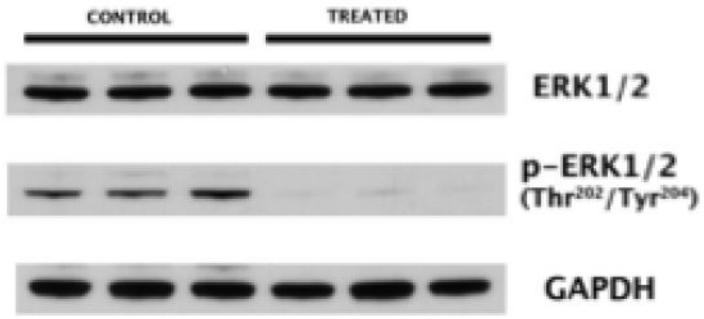

Figure 4.
Pharmacodynamics of AZD6244, western blot analysis of OS-33 xenografts treated with either vehicle or AZD6244 at 100mg/kg BID for 5 days. Tumors were harvested 1 hour after the first dose on day 5.

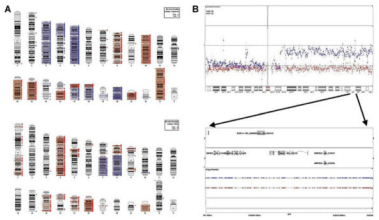

Figure 5.

Copy number analysis of BT-35 and BT-40 xenografts. Copy number analysis of BT-35 and BT-40 xenografts. Panel A. Ideograms of xenograft genomes. Genomic segments of at least 100 kb with copy gain (blue triangles) or loss (red triangles) for BT-35 (top) and BT-40 (bottom). Panel B. Copy number estimates for BT-35 (red squares) and BT-40 (blue squares) on chromosome 7 (top) and Hidden Markov model copy number states for the BRAF locus at 7q34 (bottom).

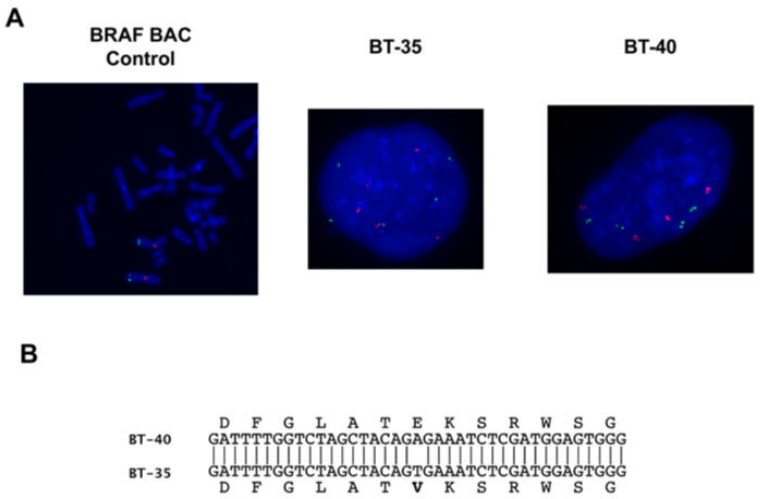

Figure 6.

Chromosome 7 duplication and BRAF sequence analysis. Panel A. Fluorescence in situ hybridization (FISH). Centromeric probes (red) and BRAF probes (Green) for normal fibroblasts, BT-35 and BT-40 xenografts. Panel B. Sequence analysis for BRAF in BT-35 and BT-40 xenografts

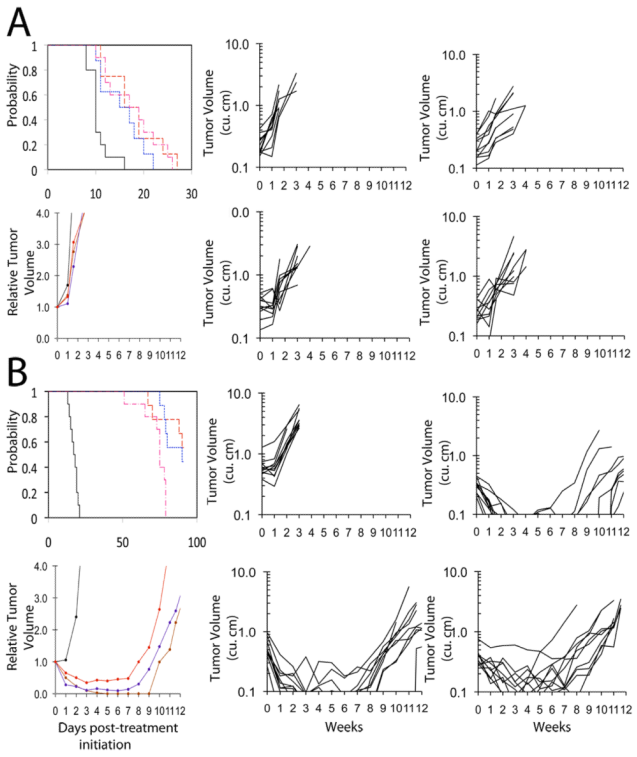

Figure 7.

AZD6244 activity against pilocytic astrocytoma xenografts. Kaplan-Meier curves for EFS, median relative tumor volume graphs, and individual tumor volume graphs are shown for (A): BT-35 and (B) BT-40. Kaplan-Meier: Controls: black solid line; 100 mg/kg BID × 5/SID × 2 for six consecutive weeks: broken red line; 75 mg/kg BID × 5/SID × 2 for six consecutive weeks: blue broken line: 100 mg/kg SID for six consecutive weeks: broken pink line. Relative Tumor Volume curves: Controls: black solid line; 100 mg/kg BID × 5/SID × 2 for six consecutive weeks: solid brown line; 75 mg/kg BID × 5/SID × 2 for six consecutive weeks: solid blue line: 100 mg/kg SID for six consecutive weeks: solid red line. For individual growth curve plots: Upper left panel: Control; Upper right panel: AZD6244 100 mg/kg BID × 5/SID × 2 for six consecutive weeks; lower left panel: AZD6244 75 mg/kg BID × 5/SID × 2 for six consecutive weeks; Lower right panel100 mg/kg SID for six consecutive weeks

Table I

Activity of AZD6244 against Cell Lines in the PPTP *in Vitro* Panel

Cell Line	Status	Histology	Minimum T/C (%)	EC_{50} (nM)	IC_{50} (nM)	BRAF Status*	RAS (Amino acid position)
RD		Rhabdomyosarcoma	29.0	122	430	Wild Type	NRAS (p.Q61H)
Rh41	Post-Therapy	Rhabdomyosarcoma	71.5	>10,000	>10,000		
Rh18	Diagnosis	Rhabdomyosarcoma	27.2	1427	1433	Wild Type	
Rh30	Diagnosis	Rhabdomyosarcoma	82.1	>10,000	>10,000	Wild Type	
BT-12	Diagnosis	Rhabdoid	69.7	>10,000	>10,000		
CHLA-266	Diagnosis	Rhabdoid	61.4	>10,000	>10,000		
TC-71 [1]	Post-Therapy	Ewing	81.8	>10,000	>10,000		
CHLA-9	Diagnosis	Ewing	69.2	>10,000	>10,000		
CHLA-10	Post-Therapy	Ewing	75.4	>10,000	>10,000		
CHLA-258	Post-Bone Marrow Transplant	Ewing	75.1	>10,000	>10,000		
SJ-GBM2	Post-Therapy	Glioblastoma	67.3	>10,000	>10,000		
NB-1643	Diagnosis	Neuroblastoma	98.6	>10,000	>10,000		
NB-EBc1	Post-Therapy	Neuroblastoma	39.9	36	356		
CHLA-90	Post-Bone Marrow Transplant	Neuroblastoma	52.1	>10,000	>10,000		
CHLA-136	Post-Bone Marrow Transplant	Neuroblastoma	81.1	>10,000	>10,000		
COG-LL-317	Post-Therapy	ALL T-cell	68.2	>10,000	>10,000		
NALM-6	Post-Therapy	ALL B-precursor	72.1	>10,000	>10,000	Wild Type	Wild Type
RS4;111	Post-Therapy	ALL B-precursor	100.0	>10,000	>10,000	Wild Type	Wild Type
MOLT-4	Post-Therapy	ALL T-cell	41.5	149	3450	Wild Type	**NRAS (p.G12C)**
CCRF-CEM		ALL T-cell	93.6	>10,000	>10,000	Wild Type	**KRAS (p.G12D)**
Kasumi-1 **	Post-Bone Marrow Transplant	AML	2.4	199.91	200	Wild Type	Wild Type
Karpas-299	Post-Therapy	ALCL	52.6	>10,000	>10,000	Wild Type	Wild Type
Ramos-RA1		NHL	94.5	>10,000	>10,000	Wild Type	Wild Type
Median			**29.0**	**>10,000**	**>10,000**		

Cell Line	Status	Histology	Minimum T/C (%)	EC_{50} (nM)	IC_{50} (nM)	BRAF Status*	RAS (Amino acid position)
Minimum			**71.5**	**36**	**200**		
Maximum			**27.2**	**>10,000**	**>10,000**		

* Mutation status from COSMIC (http://www.sanger.ac.uk/genetics/CGP/cosmic/). Blank cells have unknown mutational status;

** Has activating mutation in **KIT** (p.N822K).

Table II

Activity for AZD6244 against the PPTP *in Vivo* Panel

Xenograft Line	Histology	Kaplan-Meier Estimate of Median Time to Event	P-value[1]	EFS T/C	Median Final Relative Tumor Volume (RTV)	Tumor Volume T/C	P-Value[2]	T/C Volume Activity	EFS Activity	Response Activity
BT-29	Rhabdoid	18.7	<0.001	1.8	>4	0.43	0.005	Int	Low	Int
KT-14	Rhabdoid	22.1	0.668	1.1	>4	0.95	0.739	Low	Low	Low
KT-12	Rhabdoid	17.3	0.104	1.4	>4	0.86	0.447	Low	Low	Low
KT-10	Wilms	9.6	0.759	1.2	>4	0.96	0.971	Low	Low	Low
KT-11	Wilms	10	0.229	1.2	>4	0.73	0.258	Low	Low	Low
KT-13	Wilms	9.6	0.582	1	>4	0.93	0.965	Low	Low	Low
SK-NEP-1	Ewing	6.6	0.368	1.3	>4	0.75	0.218	Low	Low	Low
EW5	Ewing	10.8	0.317	0.9	>4	1.19	0.247	Low	Low	Low
EW8	Ewing	9.8	0.246	1.1	>4	0.95	0.684	Low	Low	Low
TC-71	Ewing	8.6	0.166	1.2	>4	0.83	0.353	Low	Low	Low
CHLA258	Ewing	10.3	0.883	0.8	>4	1.19	0.353	Low	Low	Low
Rh28	ALV RMS	31.5	0.299	1.9	>4	0.7	0.315	Low	Low	Int
Rh30	ALV RMS	18.6	0.002	1.4	>4	0.65	0.007	Low	Low	Low
Rh30R	ALV RMS	22.8	0.747	1	>4	0.88	0.912	Low	Low	Low
Rh65	ALV RMS	21.5	0.482	1	>4	0.97	0.853	Low	Low	Low
Rh18	EMB RMS	13	0.06	1.1	>4	0.94	0.360	Low	Low	Low
Rh36	EMB RMS	13.9	0.486	0.8	>4	1.13	0.393	Low	Low	Low
BT-28	Medulloblastoma	5.1	0.35	1	>4	0.87	0.315	Low	Low	Low
BT-45	Medulloblastoma	11.8	0.112	0.8	>4	1.1	0.436	Low	Low	Low
BT-46	Medulloblastoma	7	0.582	0.9	>4	1.05	0.853	Low	Low	Low
BT-44	Ependymoma	18.6	0.237	1	>4	1.02	0.280	Low	Low	Low
GBM2	Glioblastoma	11.1	0.139	1.2	>4	0.87	0.353	Low	Low	Low
BT-39	Glioblastoma	> EP	<0.001	>	2.9	0.4	<0.001	Int	Int	Int
D645	Glioblastoma	19	<0.001	1.9	>4	0.38	<0.001	Int	Low	Int

Xenograft Line	Histology	Kaplan-Meier Estimate of Median Time to Event	P-value[1]	EFS T/C	Median Final Relative Tumor Volume (RTV)	Tumor Volume T/C	P-Value[2]	T/C Volume Activity	EFS Activity	Response Activity
D456	Glioblastoma	8.9	0.011	1.3	>4	0.77	0.015	Low	Low	Low
NB-SD	Neuroblastoma	32.5	0.003	1.3	>4	0.55	0.113	Low	Low	Low
NB-1771	Neuroblastoma	34.3	0.996	1	>4	0.85	0.182	Low	Low	Low
NB-1691	Neuroblastoma	15.2	0.09	1.2	>4	0.68	0.280	Low	Low	Low
NB-EBc1	Neuroblastoma	11.4	0.916	1	>4	0.86	0.863	Low	Low	Low
CHLA-79	Neuroblastoma	15.8	0.302	1.2	>4	0.61	0.165	Low	Low	Low
NB-1643	Neuroblastoma	27.6	0.004	1.4	>4	0.37	0.007	Int	Low	Low
OS-1	Osteosarcoma	> EP	<0.001	>	3.4	0.55	<0.001	Low	Int	Int
OS-2	Osteosarcoma	19.1	0.252	1.2	>4	0.77	0.007	Low	Low	Low
OS-17	Osteosarcoma	31	0.025	1.5	>4	0.74	0.113	Low	Low	Int
OS-9	Osteosarcoma	25.9	0.091	1.1	>4	0.87	0.105	Low	Low	Low
OS-33	Osteosarcoma	36.4	<0.001	4.9	>4	0.56	<0.001	Low	Int	Int
OS-31	Osteosarcoma	16.1	0.287	1.2	>4	0.76	0.182	Low	Low	Low
ALL-2	ALL B-precursor	10.6	0.01	0.8	>25	.	.		Low	Low
ALL-3	ALL B-precursor	29.2	0.096	5.1	>25	.	.		Low	Int
ALL-4	ALL B-precursor	4.1	0.225	0.9	>25	.	.		Low	Low
ALL-7	ALL B-precursor	9.5	0.149	1.4	>25	.	.		Low	Low
ALL-16	ALL T-cell	26.2	0.13	1.6	>25	.	.		Low	Low
ALL-19	ALL B-precursor	4.2	0.208	4.2	>25	.	.		Low	Int

[1] P-value for EFS distribution for treated versus control;

[2] P-value for tumor volume Tumor Volume T/C for treated versus control.